Journal of Dynamic Systems, Measurement, and Control

Technical Briefs

Time-Energy Optimal Control of Articulated Systems With Geometric Path Constraints

Zvi Shiller[1]

The motions of articulated systems along specified paths are optimized to minimize a time-energy cost function. The optimization problem is formulated in a reduced two-dimensional state space and solved using the Pontryagin maximum principle. The optimal control is shown to be smooth, as opposed to the typically discontinuous time optimal control. The numerical solution is obtained with a gradient search that iterates over the initial value of one co-state. Optimal trajectories are demonstrated numerically for a two-link planar manipulator and experimentally for the UCLA Direct Drive Arm. The smoother time-energy optimal trajectory is shown to result in smaller tracking errors than the time optimal trajectory.

1 Introduction

Most of the recent work on optimizing the motions of articulated systems has focused on minimizing motion time, considering rigid body dynamics and treating the actuator torques/forces as the control inputs (for example see Bobrow et al., 1985, Shiller and Dubowsky, 1989). While time optimal control is relatively easy to compute due to its simple structure, the typical discontinuities at the switching times make it physically unrealizable and undesirable since: 1) actuator dynamics make a true bang-bang torque/force control impossible to implement, particularly for direct drive motors with large electrical time constants, 2) the sharp switches of the control may induce structural vibrations, and 3) the abrupt changes in the motor current may damage electric motors with permanent magnets (Kenjo and Nagamori, 1985).

Some of these practical difficulties can be addressed by modeling the actuator dynamics (Tarkiainen and Shiller, 1993). However, this increases the required computational effort because of the increased dimensionality of the system model. Alternatively, the control can be smoothed by minimizing an energy function, quadratic in the control, in addition to time (Jacobson and Speyer, 1971, Chen and Desrochers, 1988). Mathematically, this convexifies the Hamiltonian with respect to the control, creating a minimum that is not necessarily on the control boundaries.

Previous efforts for solving the energy optimization problem include a dynamic programming search in the state space for point to point motions (Vukobratovic and Kircanski, 1982) and for motions along specified paths (Shin and McKay, 1986; Singh and Leu, 1987; Pfeiffer and Johanni, 1987). The drawbacks of dynamic programming are the rapid increase in the numerical complexity with respect to the number of states (the "dimensionality curse"), and the nonsmoothness of the trajectory due to the discrete grid representation. In addition, the dynamic programming approach does not offer any a priori insights into the structure of the optimal solution. The Pontryagin maximum principle was used in (Gourdeau and Schwartz, 1989) to minimize time-energy for point to point motions. However, the point to point problem was found to be computationally difficult for higher than two degree-of-freedom manipulators.

In this paper, we solve the minimum time-energy problem for articulated systems moving along specified paths. Applying the path equality constraints, the problem is reduced to a two dimensional state space. This facilitates an efficient numerical solution that is applicable to articulated systems with any number of degrees-of-freedom. Using the Pontryagin maximum principle, the optimal control is shown to be continuous, with gradual transitions between the actuator extremes. The optimal trajectory is computed by solving a fourth-order two point boundary value problem, iterating on the initial value of a single costate. Optimal trajectories are demonstrated numerically for a two link manipulator and experimentally for the UCLA Direct Drive Arm. The time-energy optimal trajectory is demonstrated experimentally to yield smaller tracking errors than the time optimal trajectory, when used as the reference input to the PD joint controllers.

2 Problem Formulation

We consider rigid body articulated systems, modeled by the following equations of motion, simplified to exclude the gravity forces (although including gravity does not represent any conceptual difficulty in this problem)

$$\mathbf{M}(\boldsymbol{\theta})\ddot{\boldsymbol{\theta}} + \dot{\boldsymbol{\theta}}^T\mathbf{C}(\boldsymbol{\theta})\dot{\boldsymbol{\theta}} = \mathbf{T} \tag{1}$$

where $\mathbf{M}(\boldsymbol{\theta})$ is the $n \times n$ inertia matrix, $\mathbf{C}(\boldsymbol{\theta})$ is an $n \times n \times n$ array of the coefficients of the centrifugal and Coriolis forces, $\mathbf{T} \in \mathcal{R}^n$ is the vector of actuator efforts, $\boldsymbol{\theta} \in \mathcal{R}^n$, $\dot{\boldsymbol{\theta}}$, and $\ddot{\boldsymbol{\theta}}$, are the joint displacements, velocities and accelerations, respectively. The actuator efforts, $\mathbf{T}$, belong to the feasible set, Ω, defined as

$$\Omega = \{\mathbf{T} \,|\, T_{i\min} \le T_i \le T_{i\max};\ i = 1, 2, \ldots, n\} \tag{2}$$

To minimize motion time of system (1) along a specified path and ensure smooth optimal control, we solve the following optimization problem.

[1] Department of Mechanical and Aerospace Engineering, University of California Los Angeles, Los Angeles, CA 90095.

Contributed by the Dynamic Systems and Control Division of THE AMERICAN SOCIETY OF MECHANICAL ENGINEERS. Manuscript received by the DSCD June, 1993; revised manuscript received August 1994. Associate Technical Editor: H. Kazerooni.

2.1 Problem I

$$\min_{T\in\Omega} J = \int_0^{t_f} (1 + \epsilon^2 \mathbf{T}^2) dt \tag{3}$$

where t_f is the free final time, and ϵ is a weighting factor, subject to system dynamics (1), the boundary conditions

$$\boldsymbol{\theta}(0) = \boldsymbol{\theta}_0, \ \boldsymbol{\theta}(t_f) = \boldsymbol{\theta}_{t_f} \tag{4}$$

$$\dot{\boldsymbol{\theta}}(0) = \dot{\boldsymbol{\theta}}(t_f) = 0$$

and path constraints

$$\mathbf{q}(\boldsymbol{\theta}) = 0; \quad \mathbf{q} \in \mathcal{R}^{n-1}; \quad \boldsymbol{\theta} \in \mathcal{R}^n \tag{5}$$

The $n - 1$ path constraints (5) can be used to rewrite system dynamics (1) in terms of the velocity, $\dot{s}$, and acceleration, $\ddot{s}$, along the path (see Bobrow et al., 1985, Shiller and Lu, 1992, for a detailed discussion of this transformation)

$$\mathbf{m}(s)\ddot{s} + \mathbf{b}(s)\dot{s}^2 = \mathbf{T} \tag{6}$$

where $\mathbf{m}(s)$ and $\mathbf{b}(s)$ are the coefficients of the acceleration and Coriolis forces expressed in path coordinates (Shiller and Lu 1992). The transformed dynamics (6) represent a linear mapping from the actuator efforts, $\mathbf{T}$, to the acceleration, $\ddot{s}$. Since this mapping is unique (due to the linearity of (6) in both $\mathbf{T}$ and $\ddot{s}$), we can use $\ddot{s}$ as the control input, and thus reduce the n dependent control variables to an independent scalar control. This also reduces the $2n$ dimensional state space to the two independent states s (the distance along the path) and $\dot{s}$.

The reduction of the state space transforms the actuator constraints (2) to constraints on $\dot{s}$ and $\ddot{s}$ (Shiller and Lu, 1992):

$$\dot{s} \le \dot{s}_{\max}(s) \tag{7}$$

$$\ddot{s}_d(\dot{s}, s) \le \ddot{s} \le \ddot{s}_a(\dot{s}, s) \tag{8}$$

where

$$\dot{s}^2_{\max}(s) = \min_{ij} \left\{ \max_{T_i,T_j} \left(\frac{m_j T_i - m_i T_j}{m_j b_i - m_i b_j} \right) \right\}, \ i, j = 1, \ldots, n \tag{9}$$

and

$$\ddot{s}_a(\dot{s}, s) = \min_i \left\{ \max_{T_i} \left(\frac{T_i - b_i \dot{s}_2}{m_i} \right) \right\} i = 1, \ldots, n \tag{10}$$

$$\ddot{s}_d(\dot{s}, s) = \max_i \left\{ \min_{T_i} \left(\frac{T_i - b_i \dot{s}_2}{m_i} \right) \right\}, \ i = 1, \ldots, n \tag{11}$$

Denoting $\mathbf{x} = \{x_1, x_2\}^T \equiv \{s, \dot{s}\}^T$ and $u \equiv \ddot{s}$, we can now restate Problem I in the reduced state space, considering the state dependent control constraints (8) and the state inequality constraint (7).

2.2 Problem II

$$\min_u J = \int_0^{t_f} L(\mathbf{x}, u) dt \tag{12}$$

where $L(\mathbf{x}, u)$ is obtained by substituting (6) into (3)

$$L(\mathbf{x}, u) = 1 + \epsilon^2(\mathbf{b}^T\mathbf{b}x_2^4 + 2\mathbf{m}^T\mathbf{b}x_2^2 u + \mathbf{m}^T\mathbf{m}u^2) \tag{13}$$

subject to the double integrator

$$\dot{\mathbf{x}} = \mathbf{f}(\mathbf{x}, u) = [x_2, u]^T \equiv [\dot{s}, \ddot{s}]^T \tag{14}$$

the boundary conditions

$$x_1(0) = 0, \quad x_1(t_f) = s_f, \quad x_2(0) = x_2(t_f) = 0, \tag{15}$$

the state dependent control constraints (8)

$$g_1(\mathbf{x}, u) = u - u_{\max}(\mathbf{x}) \le 0 \tag{16}$$

$$g_2(\mathbf{x}, u) = u_{\min}(\mathbf{x}) - u \le 0 \tag{17}$$

and the state inequality constraint (7)

$$h(\mathbf{x}) = x_2 - \dot{s}_{\max}(x_1) \le 0 \tag{18}$$

where $u_{\max}(\mathbf{x}) \equiv \ddot{s}_a(\dot{s}, s)$ and $u_{\min}(\mathbf{x}) \equiv \ddot{s}_d(\dot{s}, s)$.

The reduction to a smaller state space allows us to formulate the problem in terms of a scalar control variable, $u(t)$. Determining the optimal control, $u^*(t)$, is equivalent to computing the optimal actuator torques $\mathbf{T}^*(t)$.

We now determine the structure of the optimal control of Problem II from the first order necessary optimality conditions for the case of state-dependent control constraints and a free final time (Bryson and Ho, 1975). We ignore the state constraint (18) since it can be shown that, excluding singular points, the state constraint is active only when the control constraints are active (Shiller and Lu, 1992). It is assumed that singularity points, as defined in (Shiller and Lu, 1992), are avoided either by appropriately choosing the path or by convexifying the set of feasible controls (Shiller 1994).

3 Structure of the Optimal Control

The solution to Problem II, $u^*(t)$, $\mathbf{x}^*(t)$, must satisfy the following necessary conditions (Bryson and Ho, 1975)

$$H_u(\mathbf{x}^*, \boldsymbol{\lambda}, u^*, t) = 0 \tag{19}$$

$$H(\mathbf{x}^*, \boldsymbol{\lambda}, u^*, t) = 0 \tag{20}$$

for all time $t \in [t_0, t_f]$, where, using (13) and (14), the Hamiltonian, $H(\mathbf{x}, \boldsymbol{\lambda}, u)$, is defined as

$$H = 1 + \epsilon^2(\mathbf{b}^T\mathbf{b}x_2^4 + 2\mathbf{m}^T\mathbf{b}x_2^2 u + \mathbf{m}^T\mathbf{m}u^2) + \lambda_1 x_2 + \lambda_2 u + \mu_1 g_1 + \mu_2 g_2 = 0 \tag{21}$$

and the co-states, $\boldsymbol{\lambda}(t)$, satisfy

$$\dot{\lambda}_1 = -2\epsilon^2\{\mathbf{m}^T\mathbf{m}_s u^2 + \mathbf{b}^T\mathbf{b}_s x_2^4 + (\mathbf{m}_s^T\mathbf{b} + \mathbf{m}^T\mathbf{b}_s)x_2^2 u\} - \mathbf{g}_s^T\boldsymbol{\mu} \tag{22}$$

$$\dot{\lambda}_2 = -4\epsilon^2(\mathbf{b}^T\mathbf{b}x_2^3 + \mathbf{m}^T\mathbf{b}x_2 u) - \lambda_1 - \mathbf{g}_{x_2}^T\boldsymbol{\mu} \tag{23}$$

The subscripts denote partial derivatives with respect to the corresponding state or control variable.

The multipliers $\boldsymbol{\mu} = [\mu_1, \mu_2]^T$ are used to append the state dependent control constraints $\mathbf{g}(\mathbf{x}, u) = [g_1(\mathbf{x}, u), g_2(\mathbf{x}, u)]^T$ ((16) and (17)) to the Hamiltonian. The multipliers, μ_1 and μ_2, are positive if the associated constraint is active, but are zero otherwise, to ensure that, at the minimum, the cost function can be reduced only by violating the constraints (Bryson and Ho, 1975). The nonzero multipliers are determined from the optimality condition (19).

Differentiating (21) with respect to u and equating to zero yields the unconstrained (interior) optimal control, $\mathbf{u}_{\text{int}}$

$$u_{\text{int}}(t) = -\frac{2\epsilon^2\mathbf{m}^T\mathbf{b}x_2^2 + \lambda_2}{2\epsilon^2\mathbf{m}^T\mathbf{m}} \tag{24}$$

The control u_{int} is the optimal control if any of the control constraints is inactive. If, at some $t = t_1$, one control constraint becomes active, then the optimal control switches to the upper or lower bounds, $u_{\max}(t_1)$, or $u_{\min}(t_1)$, respectively. The optimal control then consists of constrained arcs, determined from (10) or (11), or interior arcs, determined from (24). The structure of the optimal control $u^*(t)$ is thus given by

$$u^*(t) = \begin{cases} u_{\max}(t) & \text{if} \quad u_{\text{int}} > u_{\max} \\ u_{\text{int}}(t) & \text{if} \quad u_{\max} \ge u_{\text{int}} \ge u_{\min}, \\ & \qquad \text{for all } t \in [t_0, t_f] \\ u_{\min}(t) & \text{if} \quad u_{\text{int}} < u_{\min} \end{cases} \tag{25}$$

The optimal control is continuous at the junction points between

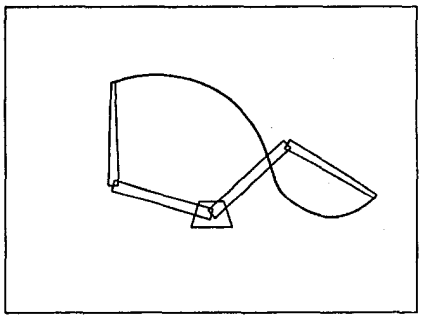

Fig. 1 A two link manipulator at the end points of a specified path

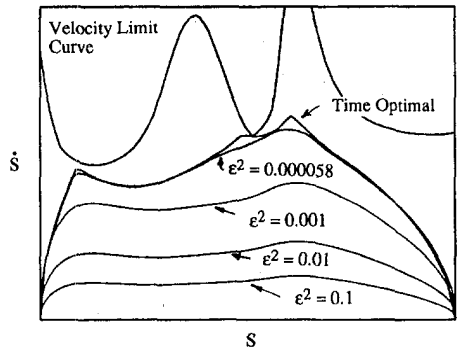

Fig. 2 Time-energy optimal trajectories in the phase plane, $s - \dot{s}$, for various values of ϵ

interior and constrained arcs due to the continuity of $\mathbf{x}$ and $\boldsymbol{\lambda}$. It follows that $\boldsymbol{\mu}$ is also continuous (and zero) across the junction points.

The interior arcs represent gradual transitions between the boundary arcs, with slopes depending on the weighting factor ϵ. As ϵ approaches zero, the transitions become sharper, and the time-energy optimal trajectory approaches the time optimal solution (Jacobson and Speyer 1971, Chen and Desrochers 1988).

4 Numerical Solution

Assuming an interior control at $t = 0$, substituting the initial condition $x_2(0) = 0$ in (21), and applying the optimality conditions (19) and (20), we eliminate one unknown by solving for the initial condition $\lambda_2(0)$

$$\lambda_2(0) = -\frac{1 + \epsilon^2 \mathbf{m}^T(0)\mathbf{m}(0)u_{\max}^2(0)}{u_{\max}(0)} \qquad (26)$$

If $u_{\text{int}}(0)$ satisfies the control constraints, then $u^*(0) = u_{\text{int}}(0)$ and the optimal trajectory starts with an interior arc. If, on the other hand, $u_{\text{int}}(0) > u_{\max}(0)$, then $u^*(0) = u_{\max}(0)$, and the optimal trajectory begins with a constrained arc. The trajectory switches to an interior arc at some time t_1 when $u_{\text{int}}(t_1)$ (24) no longer violates the actuator constraints (16) or (17).

The optimization problem thus reduces to determining the unknown initial condition $\lambda_1(0)$ to satisfy the terminal conditions (15). The selection of $\lambda_1(0)$ is essentially a line optimization problem that can be solved efficiently. It is quite computationally inexpensive compared to the dynamic programming search used in (Shin and McKay, 1986; Singh and Leu, 1987; Vukobratovic and Kircanski, 1982).

5 Examples

5.1 A Two-Link Planar Manipulator. In this example, the manipulator moves along the specified path shown in Fig. 1. The parameters of the manipulator are given in Table 1. Figure 2 shows a family of time-energy optimal trajectories in the phase plane, $s - \dot{s}$, for various values of ϵ. Also shown in Fig. 2 is the time optimal trajectory. Clearly, as ϵ approaches zero, the corresponding trajectory approaches the time optimal one. The actuator torques for the time-energy optimal solution with $\epsilon^2 = 0.0076$ and for the time optimal trajectories are shown in Fig. 3. Note the continuous transitions between the actuator extremes for the time-energy optimal trajectory. Also shown is the multiplier μ, which is continuous and nonzero whenever

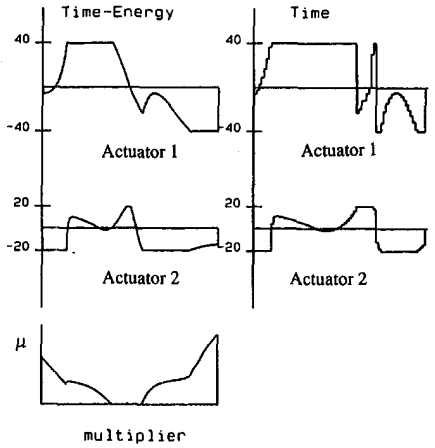

Fig. 3 Actuator torques for $\epsilon^2 = 0.000058$ and for the time optimal trajectory

one of the actuators is saturated. Here μ represents both μ_1 and μ_2 since only one of the control constraints (16) and (17) is active at one time.

For small ϵ, it is generally difficult to select an initial guess for $\lambda_1(0)$ because of the steep slopes of the interior arcs, which makes the integration highly sensitive to the initial conditions. Trajectories for a small ϵ can be computed by solving the problem repeatedly for progressively smaller ϵ's, using the solution for $\lambda_1(0)$ at each iteration as the initial guess for the next iteration. This approach was used to compute the solutions shown in Fig. 2. The motion times for various values of ϵ are shown in Fig. 4, suggesting a diminishing return for very small ϵ's.

5.2 The UCLA Direct Drive Arm. The time-energy optimal trajectories were implemented on the UCLA Direct Drive Arm shown in Fig. 5. Its controller consists of two independent PD joint controllers, each wrapped around a PD velocity control loop. The velocity controller generates the control signal to the motor driver, which in turn generates the alternating currents to the three phase motor. The optimal trajectory (position as a function of time), which was computed off-line, was used as a reference trajectory to the position controllers. Ignoring motor and driver dynamics, we used the control signal generated by the velocity loop to indicate the applied actuator torques.

Table 1 Parameters of the two-link manipulator

Link length	C.G.	Mass	Inertia around C.G.	Torque limit
$l_1 = 1.0$ m	$lc_1 = 0.5$ m	$m_1 = 1$ kg	$I_1 = 0.08$ Kg-m^2	$Q_1 = 40$ N-m
$l_2 = 1.0$ m	$lc_2 = 0.5$ m	$m_2 = 1$ kg	$I_2 = 0.08$ Kg-m^2	$Q_2 = 20$ N-m

In this example, the manipulator tip traverses the path shown in Fig. 6. Figure 7 shows the nominal and actual tip velocities for the time optimal and the time-energy optimal ($\epsilon^2 = 0.005$) trajectories, with the corresponding times of $t_{e-opt} = 0.628s$ and $t_{t-opt} = 0.547s$. As expected, the time-energy optimal trajectory is smooth, and stays below the time optimal trajectory. Figure 8 shows the tracking errors along the path for each trajectory. The nominal and actual actuator torques are shown in Figs. 9 and 10. The noted bias between the nominal and the actual torque is mainly due to the unmodeled motor friction.

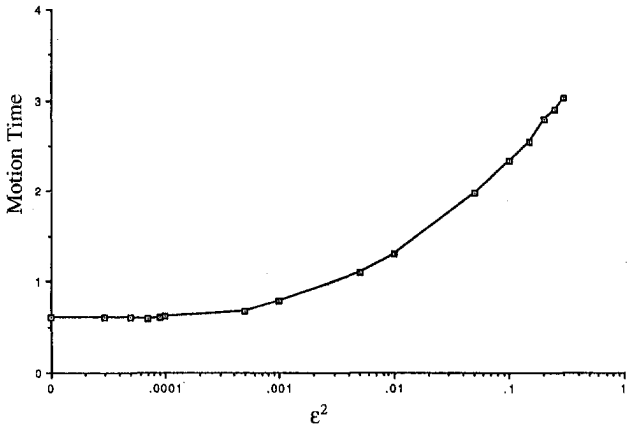

Fig. 4 Motion time versus ϵ^2

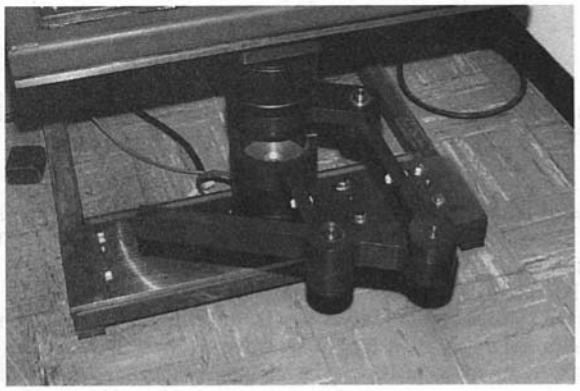

Fig. 5 The UCLA Direct Drive Arm

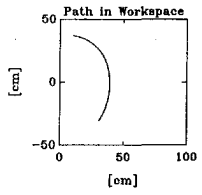

Fig. 6 The specified path in the workspace

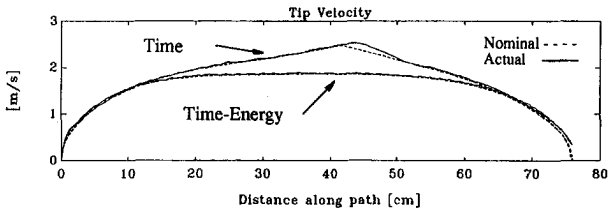

Fig. 7 The nominal and actual tip velocities for the time-optimal and time-energy optimal trajectories

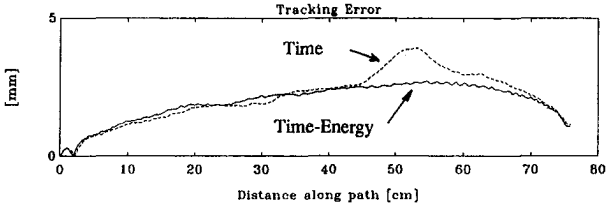

Fig. 8 The tracking errors along the path for the time-optimal and time-energy optimal trajectories

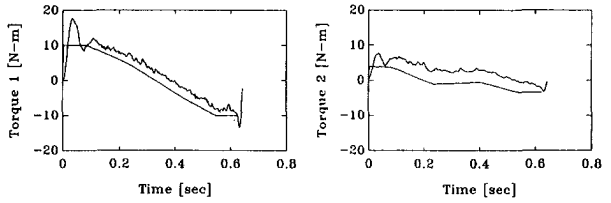

Fig. 9 The nominal and actual actuator torques for the time-energy optimal trajectory

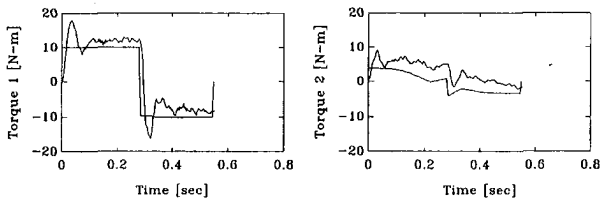

Fig. 10 The nominal and actual actuator torques for the time-optimal trajectory

The time optimal trajectory is difficult to follow due to the discontinuities in the actuator torques and the uncompensated transient dynamics of the position controller. As a result, the actual time optimal velocity profile overshoots around $s = 45$ cm, resulting in the peak tracking error of 3.9 mm, compared to the maximum error of 2.7 mm for the time-energy trajectory. The overshoot in the actual actuator torques for the first joint partly compensated for the resulting tracking error. The lower control effort and the smaller tracking errors clearly demonstrate the utility of the time-energy optimal trajectories.

6 Conclusions

A method for computing time-energy optimal trajectories along specified paths has been presented, considering the full nonlinear system dynamics and actuator constraints. The smooth trajectories produced by the time-energy cost function are demonstrated to yield better transient response and smaller tracking errors than the time optimal trajectories, when used as reference inputs to PD position controllers. In fact, the time optimal trajectory is impossible to implement without feedforward control or input preshaping (Shiller and Chang, 1995) due to the finite bandwidth of the feedback controller.

The gain in the tracking accuracy seems to outweigh the loss in motion time of the time-energy optimal trajectory. The lower control effort required to follow the time-energy optimal trajectories, and consequently, the lower motor temperature, can potentially extend the operational life of the electric motors in repetitive motions.

References

Bobrow, J. E., Dubowsky, S., and Gibson, J. S., 1985, "Time-Optimal Control of Robotic Manipulators," *Int'l J. of Robotics Research*, Vol. 4, No. 3.

Bryson, A. E., and Ho, Y. C., 1975, *Applied Optimal Control, Optimization, Estimation and Control*, Hemisphere Publishing, New York.

Chen, Y., and Desrochers, A. A., 1988, "Time-Optimal Control of Two-Degree of Freedom Robot Arms," *Proc. of IEEE Conf. on Robotics and Automation,* Philadelphia, PA, Apr., pp. 1210–1215.

Gourdeau, R., and Schwartz, H. M., "Optimal Control of a Robot Manipulator Using a Weighting Time-Energy Cost Function," *Proc. of 28th Conf. on Decision and Control,* Tampa, FL, Dec., pp. 1628–1631.

Jacobson, D. H., and Speyer, J. L., 1971, "Necessary and Sufficient Conditions of Optimality for Singular Control Problems: A Limit Approach," *J. of Mathematical Analysis and Applications* Vol. 34, No. 2, May, pp. 239–266.

Kenjo, T., and Nagamori, S., 1985, *Permanent-Magnet and Brushless DC Motors,* Clarendon Press, Oxford.

Pfeiffer, F., and Johanni, R., 1987, "A Concept for Manipulator Trajectory Planning," *IEEE Trans. Robotics and Automation,* Vol. RA-3, No. 3, pp. 115–123.

Singh, S., and Leu, M. C., 1987, "Optimal Trajectory Generation for Robotic Manipulators Using Dynamic Programming," ASME JOURNAL OF DYNAMIC SYSTEMS, MEASUREMENT AND CONTROL, Vol. 109, June, pp. 88–96.

Shiller, Z., 1994, "On Singular Points and Arcs in Path Constrained Time Optimal Motions," *IEEE Trans. on Robotics and Automation,* Vol. RA-4, No. 4.

Shiller, Z., and Chang, H., 1995, "Trajectory Preshaping of High-Speed Articulated Systems," ASME JOURNAL OF DYNAMIC SYSTEMS, MEASUREMENT, AND CONTROL, Vol. 117, No. 3, Sept., pp. 304–310.

Shiller, Z., and Dubowsky, S., 1989, "Time Optimal Path Planning for Robotic Manipulators in the Presence of Obstacles, With Actuator, Gripper and Payload Constraints," *Int'l J. of Robotics Research,* Dec., pp. 3–18.

Shiller, Z., and Lu, H. H., 1992, "Computation of Path Constrained Time Optimal Motions along Specified Paths," ASME JOURNAL OF DYNAMIC SYSTEMS, MEASUREMENT, AND CONTROL, Vol. 114, No. 3, pp. 34–40.

Shin, K. G., and McKay, N. D., 1986, "A Dynamic Programming Approach to Trajectory Planning of Robotic Manipulators," *IEEE Trans. Automatic Control,* Vol. AC-31, No. 6, pp. 491–500.

Tarkiainen, M., and Shiller, Z., 1993, "Time Optimal Motions with Actuator Dynamics," *Proceedings of IEEE Conf. on Robotics and Automation,* Atlanta, GA, May, Vol. 2, pp. 725–730.

Vukobratovic, M., and Kircanski, M., 1982, "A Method for Optimal Synthesis of Manipulation Robot Trajectories," ASME JOURNAL OF DYNAMIC SYSTEMS, MEASUREMENT, AND CONTROL, Vol. 104, June, pp. 188–193.

Adaptive Control of an Industrial Robot Retrofitted With an Open-Architecture Controller

Yuchen Zhou*,[1] and Clarence W. de Silva[1]

A PUMA 560 industrial robot has been retrofitted with an open-architecture controller. An adaptive control scheme that incorporates actuator dynamics has been implemented on this robot testbed. The overall low level control scheme is based on the complete robot-actuator dynamics, and consists of a modified regressor-based adaptive algorithm and a feedforward compensation scheme for actuator dynamics. It is shown by a Lyapunov-like analysis that, under this control scheme, the tracking error of a general robot is bounded. Experiments carried out show that the performance of the robot, with the adaptive control scheme, is significantly improved when properly compensated for actuator dynamics.

1 Introduction

It is well known that the dynamics of a robot can be represented by the set of coupled second order differential equations:

$$\mathbf{M}(\mathbf{q})\ddot{\mathbf{q}} + \mathbf{N}(\mathbf{q}, \dot{\mathbf{q}})\dot{\mathbf{q}} + \mathbf{g}(\mathbf{q}) = \boldsymbol{\tau} \tag{1}$$

where $\mathbf{q}$ is the position vector of the joints of the robot, $\boldsymbol{\tau}$ is the input force vector acting on the joints, $\mathbf{M}$ is the inertia matrix, $\mathbf{N}$ is a matrix representing the nonlinear effects such as centrifugal and Coriolis forces, and $\mathbf{g}$ denotes the gravitational forces.

The dynamics given by Eq. (1) is not necessarily a complete mathematical representation of a real robot. Difficulties in measuring inertia parameters of a robot and modeling some physical characteristics, such as joint friction, link flexibility and backlash, are reasons for the inaccuracy of the model (Book, 1984; de Silva and Shibly, 1991). Some advanced control schemes for robots have been developed that do not use their exact dynamics. Among them are variable structure control (Young, 1978; Slotine, 1983), and several types of adaptive control (Dubowsky et al., 1979; Landau, 1979; Craig, 1986; de Silva, 1987; Slotine, 1987). Both approaches are effective in dealing with dynamic uncertainties and external disturbances.

Most control schemes available to date exclude actuator dynamics simply by assuming that the required control torques can be generated at the robot joints. This assumption is not valid for most industrial robots driven by electrical motors. Usually a voltage signal is generated and applied to the armature of the motor. The behavior of these actuators is typically governed by a third order differential equation (de Silva, 1989; Spong and Vidyasagar, 1989), that takes into account both electrical and mechanical time constants. This, when incorporated into the robot dynamics, can substantially modify the overall dynamics of the system. Dealing with the third order dynamics of a robot actuator is further plagued by the resulting presence of the time derivatives of joint forces (torques), because it is somewhat unrealistic to measure these force derivatives for control purposes. In many situations, however, the actuator dynamics will dominate the robot dynamics (Tarn, 1991), for example, when the gear reduction is large (such as in PUMA robots). This problem has been studied by some researchers, and a few control schemes have been proposed (Dawson, 1992; Ge, 1993). However, usually joint acceleration and jerk (or joint acceleration and motor current) feedback is required. This requirement brings difficulty to practical applications.

How a real robot-actuator system behaves under various advanced control schemes is of great importance in practical robot applications, and this is the motivation of the present work. This paper studies the performance of an industrial robot under an adaptive control scheme which incorporates actuator dynamics. Based on a complete robot-actuator dynamic model which uses the reduced order actuator dynamics, a modified parameter-linearization adaptive control with feedforward compensation, is then designed. The proposed control scheme does not require acceleration or jerk or current feedback. Through a Lyapunov-like analysis, it is shown that under this control scheme, the tracking error of a robot is bounded, and this bound is computable and depends on the estimation error. In the ideal case of perfect estimation, the tracking error will asymptotically converge to zero. Experiments carried out on a PUMA 560 robot show that the proposed control scheme can improve the performance of the robot in a significant manner.

2 Adaptive Control Scheme

2.1 Actuator Dynamics. It is assumed that the robot is actuated by permanent magnet DC motors. The dynamics of such a motor for joint j is given by (de Silva, 1989; Dawson et al., 1992)

$$L_{a,j}\frac{di_{a,j}}{dt} + R_{a,j}i_{a,j} + K_{b,j}\frac{d\theta_{m,j}}{dt} = v_{a,j} \tag{2}$$

where $L_{a,j}$ is the armature leakage inductance, $R_{a,j}$ is the arma-

*Presently with Institute for Advanced Manufacturing Technology, National Research Council, Ottawa, Canada.

[1] Industrial Automation Laboratory, Department of Mechanical Engineering, University of British Columbia, Vancouver, B.C., V6T 1Z4, Canada. Dr. de Silva is a Fellow ASME.

Contributed by the Dynamic Systems and Control Division of THE AMERICAN SOCIETY OF MECHANICAL ENGINEERS. Manuscript received by the DSCD April 12, 1994; revised manuscript received November 28, 1994. Associate Technical Editor: B. Siciliano.